Antarct. Meteorite Res., **18**, 253–272, 2005

Chondrule age distribution and rate of heating events for chondrule formation

Taishi Nakamoto[1]*, Noriko T. Kita[2,3] and Shogo Tachibana[4]

[1] *University of Tsukuba, Center for Computational Sciences, Tsukuba 305-8577*
[2] *Department of Geology and Geophysics, University of Wisconsin, U.S.A.*
[3] *Geological Survey of Japan, AIST, Tsukuba 305-8567*
[4] *University of Tokyo, Department of Earth and Planetary Science, Bunkyo-ku, Tokyo 113-0033*
**Corresponding author. E-mail: nakamoto@rccp.tsukuba.ac.jp*

(Received September 15, 2004; Accepted January 21, 2005)

Abstract: Chondrules are considered to be formed by flash heating events in the protoplanetary disk. In order to evaluate some basic factors in the heating mechanism, we examined the rate of heating events that explains the abundance and the observed age distribution of chondrules in unequilibrated ordinary chondrites. First, we compiled the literature data of ^{26}Al ages of chondrules from the least equilibrated ordinary chondrites (LL3.0–3.1), ranging from 1 Myr to 3 Myr with a peak at about 1.8 Myr relative to the formation time of Ca, Al-rich inclusions (CAIs) in carbonaceous chondrites, the oldest solid materials formed in the solar system. Next, we made a simple phenomenological chondrule formation model assuming that each event heated only a small fraction of existing dust at one time and numerous heating events produced chondrules. Results indicate that (1) an average number of heating events experienced by a dust particle should be 1.2 or higher, (2) more than a half of the present chondrules were reheated, (3) chondrule formation started sometime between 0.4–1.5 Myr and ended at 2.2–2.3 Myr after the CAI formation, and (4) the rate of heating events has a peak at 0.1–0.8 Myr earlier than the peak of the observed chondrule age distribution and should decrease monotonically with time after the peak.

key words: chondrules, origin, solar system, solar nebula, thermal histories

1. Introduction

Chondrules, which are mm-sized silicate igneous spheres contained in chondrites, are believed to have formed through flash heating events in the early solar system (*e.g.*, Jones *et al*., 2000 and references therein). Some chondrules are considered to be preserved in small asteroidal bodies without significant alteration and metamorphism since their formation. By investigating the formation process of such chondrules one can reveal the nature of the early solar system. Several heating mechanisms for chondrule formation have been proposed to date: among them are bipolar outflow (Liffman, 1992; Shu *et al*., 1996), nebular lightning (Morfill *et al*., 1993; Eisenhour *et al*., 1994), clumpy cloud accretion shocks (Boss and Graham, 1993; Hood and Kring, 1996; Tanaka *et al*., 1998), shock waves in a dusty zone in the nebula (Hood and Horanyi, 1991, 1993), and planetesimal bow shocks (Hood, 1998; Weidenschilling *et al*., 1998). As summarized in Boss (1996), none of these models has been accepted widely so far, except for the shock wave heating mechanism that successfully explains many properties of chondrules (*e.g.*, Connolly and Love, 1998) and is considered by many authors as the most promising mechanism for chondrule formation (Wood, 1963; Stolper and Paque, 1986; Hood and Horanyi, 1991, 1993; Hood and Kring, 1996; Boss, 1996; Hood, 1998; Tanaka *et al.*, 1998; Weidenschilling *et al.*, 1998; Iida *et al.*, 2001; Susa and Nakamoto, 2002; Desch and Connolly, 2002; Miura *et al.*, 2002; Ciesla and Hood, 2002; Sekiya *et al.*, 2003; Miura and Nakamoto, 2005a, b). Specifying the chondrule forming mechanism should provide significant implications regarding the physical conditions of the early solar system where chondrules formed.

In spite of numerous detailed studies on the properties of chondrules, we still lack a general picture of the heating events. For example, the total amount of energy consumed to form chondrules and the spatial distribution of the heating events are not yet well constrained from chondrule studies, primarily because we do not know whether chondrule forming processes were localized in the asteroid regions (where meteorite parent bodies are considered to be formed) or were common throughout the protoplanetary disk. On the other hand, formation ages of chondrules indicate the time-scale and frequency of the heating events and may help us specify the heating mechanism of chondrule formation. Small excesses of ^{26}Mg from decay of the short-lived radionuclide ^{26}Al with a half-life of 0.73 million years (Myr) have been detected from Al-rich phases in chondrules (*e.g.*, Hutcheon and Hutchison, 1989; Russell *et al.*, 1996). The initial ^{26}Al/^{27}Al ratio when the ^{26}Al-^{26}Mg system in a chondrule became closed is estimated from the observed ^{26}Mg excesses that correlate with ^{27}Al/^{24}Mg ratios. Measurements have been made on numerous chondrules from the unequilibrated ordinary chondrites (UOCs, LL3.0–3.1) and their initial ^{26}Al/^{27}Al ratios range between 2×10^{-5} and 3×10^{-6} (Hutcheon and Hutchison, 1989; Kita *et al.*, 2000; McKeegan *et al.*, 2000; Mostefaoui *et al.*, 2002). Since those UOCs are least thermally metamorphosed, the ^{26}Al-^{26}Mg systems in the chondrules have not been disturbed on their parent bodies and thus became closed at the time of chondrule heating event. The range of the initial ^{26}Al/^{27}Al ratios for chondrules corresponds to relative ages of 1 Myr to 3 Myr after the formation of Ca, Al-rich inclusions (CAIs), the oldest solid materials in the solar system, which have the canonical initial ^{26}Al/^{27}Al ratios of 5×10^{-5} (MacPherson *et al.*, 1995). The mean life of ^{26}Al is nearly 1 Myr. The errors of the relative ages are usually 1 Myr or less (0.2 Myr for the best measurements). Thus, we can now apply the age distribution of chondrules to discuss a time-variation of the chondrule-forming heating mechanism.

Hereafter a time of zero is assigned to the time of CAI formation. The word "age" refers to time of formation after $t=0$ and represents the timing when the ^{26}Al-^{26}Mg system became closed. "Young" chondrules have larger age t than "older" chondrules, because "young" chondrules formed after "older" chondrules.

It should be mentioned that the homogeneity of ^{26}Al/^{27}Al ratios in the early solar system is assumed in obtaining the above relative ages, though it has always been a matter of debate. However, the relative ^{26}Al-^{26}Mg ages obtained from the various types of meteoritic samples are found to be consistent with other chronometers, such as ^{207}Pb-^{206}Pb and ^{53}Mn-^{53}Cr ages (*e.g.*, Zinner and Göpel, 2002; Amelin *et al.*, 2002; Kita *et al*., 2003), strongly indicating the homogeneous distribution of Al isotopes in the early solar system.

Recent data for ^{26}Al-^{26}Mg systems of bulk Allende chondrules, measured by inductively coupled plasma-mass spectrometry (ICP-MS) (Bizzarro *et al*., 2004), show that some chondrules have the initial ^{26}Al/^{27}Al ratios close to the canonical value, suggesting that such chondrules formed at the same time with CAIs. However, these initial ^{26}Al/^{27}Al ratios for bulk chondrules may have been those at the time of chondrule-precursor formation rather than those at the last melting event. On the other hand, the initial ^{26}Al/^{27}Al ratios obtained from Al-rich minerals or mesostasis by ion microprobe probably record the last heating events for individual chondrules because such Al-rich phases would have been easily reset by heating events. Thus, we will not use the ^{26}Al-^{26}Mg data for bulk chondrules to discuss chondrule-heating events.

The distribution of chondrule ages may directly correlate with the history of the heating events, if each chondrule in the present meteorites formed by a single melting event from primitive dust in the solar nebula. However, we have considerable evidence for multiple heating, such as the presence of relict olivine grains obviously derived from earlier generations of chondrules (*e.g*., Nagahara, 1981; Jones, 1996). Because each chondrule would have recorded the last heating event it experienced, the age distribution of chondrules may have a peak at a younger age (*i.e*., longer time-interval from CAI formation) than the frequency distribution of heating events does. In order to draw a general picture of the heating events, we present here a simple phenomenological model for chondrule formation, and estimate a rate of heating events. The rate of heating events means the fraction of material that experiences heating events per unit time and is equivalent to a volume fraction of material in the nebula subjected to a single heating event multiplied by numbers of heating events per unit time. The chondrule formation rate would be deduced from the rate of heating events by considering a production efficiency of new chondrules and is further related to age distribution of chondrules, with a modification to take into account reheating effects. We do not specify any heating mechanism in this model, but seek the solutions that satisfy the observed age distributions for chondrules in ordinary chondrites as well as their total volume.

2. ^{26}Al-^{26}Mg age distribution of UOC chondrules

2.1. Compilation of ^{26}Al-^{26}Mg age data

We compiled the ^{26}Al-^{26}Mg ages of UOC chondrules from type 3.0–3.1 ordinary chondrites (Table 1; data sources: Hutcheon and Hutchison, 1989; Kita *et al*., 2000; McKeegan *et al*., 2000; Mostefaoui *et al*., 2002; Tomomura *et al*., 2004; Tomomura, 2004). To use the ^{26}Al-^{26}Mg system as a chronometer, the relative abundance of ^{26}Al to a stable isotope, ^{27}Al, should be constant within an object at the time of formation. Chemical fractionations of Al from Mg occur at the time of chondrule formation, forming phases with different Al/Mg ratios such as magnesian silicates and Al-rich mesostasis. After formation, the relative abundance of the daughter isotope, ^{26}Mg*, to ^{24}Mg will correlate with ^{27}Al/^{24}Mg ratios if the object remains chemically closed. From such a correlation, the initial abundance of ^{26}Al relative to ^{27}Al (^{26}Al/^{27}Al; hereafter r) is obtained. Although the absolute age of an object cannot be obtained by using

Table 1. Compilation of ^{26}Al-^{26}Mg age determination of chondrules from LL3.0–3.1.

Sample	$^{26}Al/^{27}Al$ ($\times 10^{-5}$)		Age (Myr)		Type	Ref.*
Bishunpur II-C1	2.28	±0.73	0.83	−0.29/+0.41	II AB	4
Bishunpur I-C4	1.20	±0.24	1.50	−0.19/+0.24	II AB	4, 6
Bishunpur II-C10	1.02	±0.54	1.67	−0.45/+0.79	I AB	4
Bishunpur I-C56	0.96	±0.09	1.74	−0.09/+0.10	II B	4, 6
Krymka K21	0.96	±0.13	1.74	−0.13/+0.15	IIAB	5
Semarkona 1805-C5	0.96	±0.35	1.74	−0.33/+0.48		3
Semarkona 1805-9 CH23	0.92	±0.50	1.79	−0.46/+0.83	II AB	2
Semarkona 1805-9 CH4	0.89	±0.16	1.81	−0.17/+0.20	II AB	2
Semarkona 1805-9 CH3	0.88	±0.31	1.83	−0.32/+0.45	I AB	2
Bishunpur 2359-C5	0.86	±0.56	1.85	−0.53/+1.11		3
Bishunpur I-C18	0.84	±0.39	1.88	−0.40/+0.66	II AB	4, 6
Semarkona 1805-5 CC1	0.77	±0.21	1.97	−0.25/+0.34	II AB	1
Bishunpur II-C20	0.74	±0.57	2.01	−0.60/+1.53	II AB	4
Bishunpur 2359-C8	0.71	±0.40	2.06	−0.47/+0.87		3
Semarkona 1805-9 CH36	0.66	±0.19	2.13	−0.26/+0.35	II AB	2
Krymka K27	0.61	±0.17	2.22	−0.26/+0.34	IIB	5
Bishunpur II-C18	0.57	±0.20	2.29	−0.32/+0.46	II AB	4
Bishunpur II-C7	0.55	±0.84	2.32	−0.97/**	II AB	4
Bishunpur II-C13	0.53	±0.70	2.37	−0.89/**	II B	4
Semarkona 1805-9 CH60	0.46	±0.21	2.52	−0.40/+0.65	II B	2
Bishunpur II-C12	0.45	±0.21	2.54	−0.41/+0.67	II AB	4
Bishunpur II-C17	0.35	±0.48	2.82	−0.92/**	I B	4

* [1] Hutcheon and Hutchison (1989), [2] Kita *et al*. (2000), [3] McKeegan *et al*. (2000), [4] Mostefaoui *et al*. (2002), [5] Tomomura *et al*. (2004), [6] Tomomura (2004).
** Data give only upper limits to the ages.

short-lived radionuclides, the age difference between two objects can be calculated based on their r values. The age of each chondrule (t), relative to CAIs, is calculated by using the following formula,

$$t = -\tau_{\mathrm{half}} \times \ln(r/r_0)/\ln(2), \tag{1}$$

where r_0 and τ_{half} represent the solar system initial $^{26}Al/^{27}Al$ ratio (5×10^{-5}) and the half life of ^{26}Al (0.73 Myr), respectively. Kita *et al*. (2000) and Mostefaoui *et al*. (2002) used $r_0 = 4.5\times10^{-5}$ from the average value for type-B CAIs (MacPherson *et al*., 1995). However, in most other recent publications, r_0 is taken as 5×10^{-5}, which is often referred to as the canonical value for CAIs. For this reason, we use $r_0 = 5\times10^{-5}$ in this study for consistency: this difference shifts ages by 0.11 Myr.

If a chondrule is reheated in a later heating event, either in the solar nebula or on a parent body, ^{26}Mg may be homogenized. The ^{26}Al-^{26}Mg clock restarts and dates the later heating event (age-resetting).

We do not include data from UOCs with petrologic sub-types higher than 3.3 because there is a possibility of age resetting by a mild thermal metamorphism on parent bodies (Kita *et al*., 2000; Huss *et al*., 2001). From the data set in Table 1, we obtain ages that vary between 1 Myr and 3 Myr, though many data show a large age error of >0.5 Myr, making it difficult to determine the detailed age distribution. The histogram

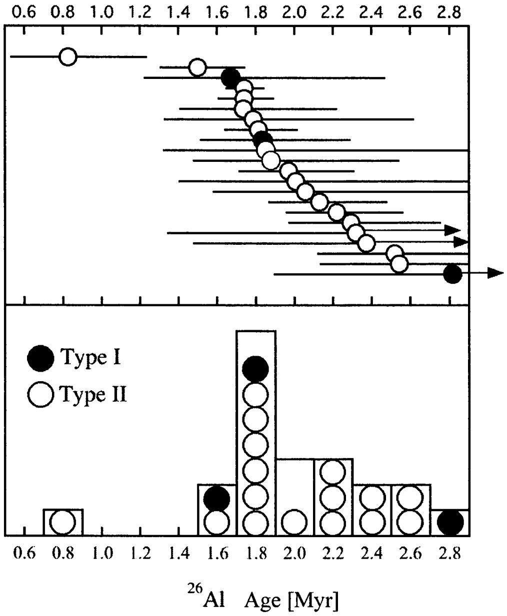

Fig. 1. Age distribution of porphyritic chondrules in LL3.0–3.1 chondrites. Data are listed in Table 1.

shown in Fig. 1 shows a peak near 1.8 Myr with a significant wide range of variation (± 1 Myr).

We consider that this age distribution, showing a peak near 2 Myr, represents the general trend among chondrules from LL chondrites. However, there is a recognized sampling bias. Most chondrules do not contain phases with high Al/Mg ratios, so ^{26}Mg excesses are generally too small (< 1‰) to be detected even using the latest analytical techniques. Existing data have been obtained from a population of chondrules that contain either plagioclase (Al/Mg > 30) and/or Al-rich glass with low Mg contents ($< 1\%$) (typically 10% of all chondrules in individual thin section; Kita *et al.*, 2000; Mostefaoui *et al.*, 2002; Tomomura *et al.*, 2004). Type IA (FeO-poor olivine-rich) chondrules, a common type of chondrules, are not included in the data set because they rarely contain high Al/Mg phases. The data set contains more type II (FeO-rich) than type I (FeO-poor) chondrules, because type II chondrules often contain glass with low Mg contents. Therefore, the distribution shown in Fig. 1 may not represent the whole population of chondrules in LL chondrites.

2.2. *Estimation of age distribution of chondrules*

Mostefaoui *et al.* (2002) first indicated that there is a correlation between ^{26}Al-ages of LL3.0–3.1 chondrules and their olivine and pyroxene contents. This was further recognized as a correlation between ^{26}Al-ages and bulk abundance of Si and volatile elements ((Si, Mn, Cr, or Na)/Mg) by Tachibana *et al.* (2003). They found that younger chondrules tend to contain more Si and volatile elements than older ones do.

The correlation line for ^{26}Al-ages and bulk (Si/Mg) ratios of chondrules reported in Tachibana *et al.* (2003) was updated by Tomomura (2004) based on 19 chondrule data including new and re-measured ^{26}Al ages as follows;

$$t = 0.543 + 1.284 \times (\mathrm{Si/Mg})_{\mathrm{molar}} / (\mathrm{Si/Mg})_{\mathrm{CI}} \text{ Myr.} \tag{2}$$

This equation implies that one may be able to estimate the formation age of a chondrule from its bulk chemical composition. Tomomura *et al.* (2004) measured bulk chemical compositions of 89 chondrules from unequilibrated ordinary chondrites (Bishunpur and Krymka, both LL3.1) without any selection biases. From the distributions of CI normarized Si/Mg ratios among these chondrules, the age distribution for porphyritic chondrules is estimated by using eq. (2) as shown in Fig. 2. We see the peak at around 1.9 Myr, which is close to the peak for the measured data. As chondrules are made of olivine, $(Fe, Mg)_2SiO_4$, and pyroxene, $(Fe, Mg) SiO_3$, as major constituents, the lowest Si/Mg ratio expected for chondrules is 0.5, a composition of forsterite (Mg_2SiO_4). By applying the Si/Mg-age relationship, we may not obtain chondrules younger than 1.2 Myr, which corresponds to Si/Mg of 0.5. Actual measured chondrule ages are also younger than 1.2 Myr ($t > 1.2$ Myr) except for rare cases.

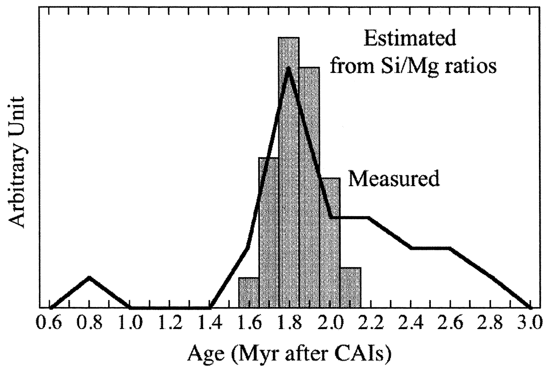

Fig. 2. The estimated age distribution of chondrules based on the correlation between ages and Si/Mg ratios. "Measured" (a solid line) indicates the distribution in Fig. 1.

The above estimated age distribution may change in detail by addition of new data with higher precision analyses, which is the on-going study (*e.g.*, Kita *et al.*, 2005) and the correlation line should be strictly evaluated by using a large number of data (*ca.* 100 data instead of 19). The correlation line is mostly controlled by the type II chondrule data so that the estimated age distribution was obtained by assuming both type I and II chondrules show the same age-Si/Mg relationship, which is not yet confirmed. Furthermore, we ignored non-porphyritic chondrules, such as barred olivine and radial pyroxene, as ^{26}Al-ages have not been obtained for these. However, they are relatively minor constituents; only ~10% and ~4% of all UOC chondrules for radial pyroxene and barred olivine chondrules, respectively (Grossman *et al.*, 1988). Tomomura *et al.* (2004) found eight radial pyroxene chondrules and one barred olivine chondrule among 89 chondrules they studied. Considering that radial pyroxene chondrules are generally

Si and Fe-rich, their Si/Mg ratios could be similar to or higher than IIB chondrules. Therefore, radial pyroxene chondrules may add some contribution to high Si/Mg chondrules.

In summary, both the measured chondrule data and the estimated age distribution by using the chondrule type frequency and the age-Si/Mg correlation indicate that the ages of chondrules are distributed between 1 Myr and 3 Myr after CAIs with a peak at 1.8–1.9 Myr. In spite that two independent estimates give similar distributions in general, a reliability of the distribution is still in question. Therefore, we conservatively mention that the present models and discussions based on the above age distribution are subject to change by future additions of high precision chondrule ^{26}Al age data.

3. Chondrule formation model

Figures 1 and 2 show that chondrule formation did not take place only once but occurred many times, at least over about 2 Myr. Petrographic evidence also shows that some chondrules experienced multiple heating (Jones, 1996). If all the pre-existing chondrules were heated and their ^{26}Al ages were reset in each chondrule-forming event, all the chondrules would have the same ^{26}Al age for the last heating event and we would not obtain the age distribution seen in Figs. 1 and 2. This indicates that each heating event formed or reheated only a small fraction of chondrules and that the total chondrule population is the result of many heating events.

In order to examine the rate of heating events, we make a simple phenomenological model for chondrule formation. We assume that all the solid material is categorized into two groups: "matrix material", which includes small dust particles that are incorporated as matrix into chondrite parent bodies later, and "chondrules". Note that "matrix material" we define here is fine dust precursors and is not necessarily matrix found in chondrites. We model the chondrule formation as follows (see Fig. 3): (1) all the material is in a closed volume where chondrule formation and destruction take place,

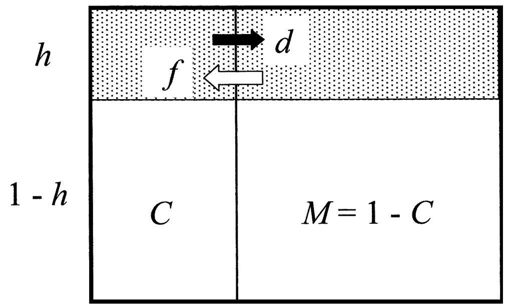

Fig. 3. A simple phenomenological chondrule formation model. All the solid material is assumed to be in a closed volume and categorized into two groups: matrix and chondrule. The fraction of chondrules is denoted by C and that of matrix is expressed by M, where $M = 1 - C$ is satisfied. In a unit time, a certain fraction of solid material, $h(t)$, is heated. A fraction of heated matrix material forms chondrules and a fraction of heated chondrules are destructed and change into matrix material.

(2) a local heating event affects only a minor fraction of material in the volume at one time, but occurs many times during the chondrule formation epoch, (3) a certain fraction of matrix material is converted to chondrule material in a chondrule forming heating event, and a certain fraction of chondrules is destroyed (or evaporated) and converted to (or recondensed as) matrix material, and (4) newly formed chondrules date the heating event. The rate of heating events, h, is defined as the fraction of the material that is affected by the heating events in a unit time.

The time derivative of the fraction of chondrules among all the solid material, C, is given by

$$\frac{\mathrm{d}C}{\mathrm{d}t}=M\cdot f-C\cdot d, \tag{3}$$

where M represents the fraction of matrix among all the solid material and $M=1-C$, f is the chondrule formation rate at which the matrix materials are converted to chondrules in a unit time, and d is the destruction rate at which the chondrules are converted to matrix particles in a unit time. Since the formation and destruction of chondrules are related to the heating events, we assume that f and d are in proportion to the rate of heating events h as $f=gh$ and $d=eh$, where g and e are formation and destruction efficiencies, respectively. We also assume that the efficiencies and are constants throughout the chondrule formation epoch, for simplicity in this study. Then the eq. (3) can be rewritten as

$$\frac{\mathrm{d}C(t)}{\mathrm{d}t}=-\left[C(t)-\frac{g}{g+e}\right](g+e)\cdot h(t). \tag{4}$$

The solution should satisfy $C(t_{\mathrm{fin}})=C_{\mathrm{fin}}$ at $t=t_{\mathrm{fin}}$ when the final chondrule formation occurred, where C_{fin} is the chondrule fraction we observe in chondrites. Then, the solution of the eq. (4) is given by,

$$C(t)=\frac{g}{g+e}+\left[C_{\mathrm{fin}}-\frac{g}{g+e}\right]\exp\left[(g+e)\int_t^{t_{\mathrm{fin}}}h(t')\mathrm{d}t'\right]. \tag{5}$$

Equation (5) has two distinctive solutions depending on the sign of $C_{\mathrm{fin}}-g/(g+c)$. When $C_{\mathrm{fin}}-g/(g+e)<0$, $C(t)$ is a monotonically increasing function of time, and more chondrules are *produced* than destroyed in heating events. On the other hand, in the case of $C_{\mathrm{fin}}-g/(g+e)>0$, $C(t)$ is a monotonically declining function, and the heating events *destroy* chondrules. However, in this case, a very high initial fraction of chondrules is required to reconcile the final chondrule fraction ($C_{\mathrm{init}}>C_{\mathrm{fin}}\approx0.7$ for ordinary chondrites), which seems unlikely in the scenario of star/planetary system formation. Hence, in this study, we assume that the condition of the heating events was the *productive* case, i.e. $C_{\mathrm{fin}}-g/(g+e)<0$.

When a heating event occurred at time t, the amount of chondrules that record the timing of the heating event ($b(t)$) is expressed by

$$b(t)=(M\cdot f+C\cdot h\cdot(1-e))=\{g+[1-(g+e)]\cdot C\}\cdot h, \tag{6}$$

where $M\cdot f$ and $C\cdot h\cdot(1-e)$ represent the formation of chondrules from the matrix and the age resetting by reheating, respectively. Since a fraction of chondrules that date the time t is reheated and their ages are reset by subsequent heating events, the amount of chondrules that have the time stamp at t decreases as time proceeds. Thus the final fraction of chondrules having the last heated time stamp t at the time of $t_{\rm fin}$ is given by,

$$y(t) = b(t)\exp\left[-\int_t^{t_{\rm fin}} h(t')\,dt'\right]. \tag{7}$$

This quantity $y(t)$ expresses the fraction of chondrules that are formed or that have their ages reset at t, after which their ^{26}Al ages have never been reset. Thus, $y(t)$ can be compared with the estimated age distribution of natural chondrules (Fig. 2).

Let us suppose that the chondrule forming heating events began at the time t_0 and ceased at the time $t_{\rm fin}$. Then, the integrated age distribution of chondrules over the time from t_0 to $t_{\rm fin}$ is the total amount of formed chondrules. This quantity, Y, is given by,

$$\begin{aligned} Y &= \int_{t_0}^{t_{\rm fin}} y(t)\,dt \\ &= \frac{g}{g+e}\left(1-\exp\left[-\int_{t_0}^{t_{\rm fin}} h(t)\,dt\right]\right) + \left(C_{\rm fin} - \frac{g}{g+e}\right)\left(1-\exp\left[-\{1-(g+e)\}\int_{t_0}^{t_{\rm fin}} h(t)\,dt\right]\right), \end{aligned} \tag{8}$$

and should be equal to $C_{\rm fin}$. The amount of chondrules, which have ages that have never been reset by reheating after their formation from matrix, S, is given by,

$$\begin{aligned} S &= \int_{t_0}^{t_{\rm fin}} M(t')f(t') \cdot \exp\left[-\int_{t'}^{t_{\rm fin}} h(t'')\,dt''\right] dt' \\ &= g \cdot \left(1 - \frac{g}{g+e}\right)\left(1-\exp\left[-\int_{t_0}^{t_{\rm fin}} h(t)\,dt\right]\right) \\ &\quad + \frac{g}{1-(g+e)}\left(\frac{g}{g+e} - C_{\rm fin}\right)\left(1-\exp\left[-\{1-(g+e)\}\int_{t_0}^{t_{\rm fin}} h(t)\,dt\right]\right). \end{aligned} \tag{9}$$

The amount of chondrules that have been reheated more than once after they first formed, *i.e.* the total amount of reheated chondrules, R, is given by

$$R = C_{\rm fin} - S. \tag{10}$$

Note that quantities Y, S, and R depend only on the time integral of $h(t)$, $\int_{t_0}^{t_{\rm fin}} h(t)\,dt$, and do not depend on the specific form of the function $h(t)$. The integration of the rate of heating events with respect to time expresses the average number of heating events that each dust particle has experienced in a time period from t_0 to $t_{\rm fin}$.

4. Results and discussion

4.1. *Total amount of heating*

The total fraction of chondrules within the total amount of solid material, Y, is given by eq. (8) as a function of the total amount of heating $\int_{t_0}^{t_{\rm fin}} h(t)\,dt$. By using the constraint $Y = C_{\rm fin}$ and solving the eq. (8) for $\int_{t_0}^{t_{\rm fin}} h(t)\,dt$, we have

$$\int_{t_0}^{t_{\rm fin}} h(t)\,dt = \frac{1}{g+e}\ln\left[\frac{1}{1-C_{\rm fin}(g+e)/g}\right]. \tag{11}$$

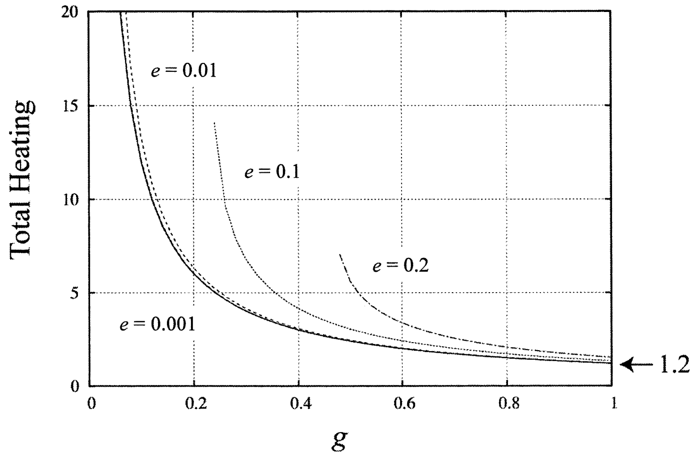

Fig. 4. Total amount of heating as a function of the production efficiency g and the destruction efficiency e. The current fraction of chondrules is assumed to be $C_{fin}=0.7$.

The total amount of heating $\int_{t_0}^{t_{fin}} h(t)\,dt$ is shown as a function of the production efficiency g with different values of the destruction efficiency e in Fig. 4. One can see that the total amount of heating should be large for the smaller g (production efficiency) in order to produce a large amount of chondrules. The total amount of heating changes significantly depending on the choice of the formation efficiency g and the destruction efficiency e. For example, if $g=0.5$ and $e=0.1$, the total amount of heating should be 3.05. This means that each solid material was heated 3.05 times on average, during the chondrule formation epoch. According to eq. (11), a lower limit for the total amount of heating of 1.2 is obtained for the most productive case where $g=1$ and $e=0$, indicating that it would be difficult for primitive unmelted dusts in the chondrule-forming region to be preserved in chondrites with abundant chondrules.

Note that we assume that the heating events are *productive* in this study, so g and e should satisfy $C_{fin}-g/(g+e)<0$, which can also be seen in eq. (11). Thus, there exists a lower limit for g that depends on e (Fig. 4). In order for heating events to be *productive*, e should satisfy $e<g\,(1-C_{fin})/C_{fin}=0.43g$ for C_{fin} of 0.7.

4.2. Fraction of reheated chondrules

The fraction of reheated chondrules among all the chondrules, R/C_{fin}, which is also obtained as a function of the total amount of heating, is displayed in Fig. 5. In panel (a), R/C_{fin} as a function of g is shown. It is seen that, when e is fixed, R/C_{fin} is high when g is small because the total amount of heating is larger for smaller g. On the other hand, in panel (b), R/C_{fin} is displayed as a function of e. When g is smaller than about 0.9, R/C_{fin} increases monotonically as e increases. This is also because the total amount of heating is larger for smaller e (see Fig. 4). When g is larger than about 0.9, the difference of the total amount of heating with different e is small (see Fig. 4), so the increment of e leads to the decrement of R/C_{fin} through the destruction of chondrules.

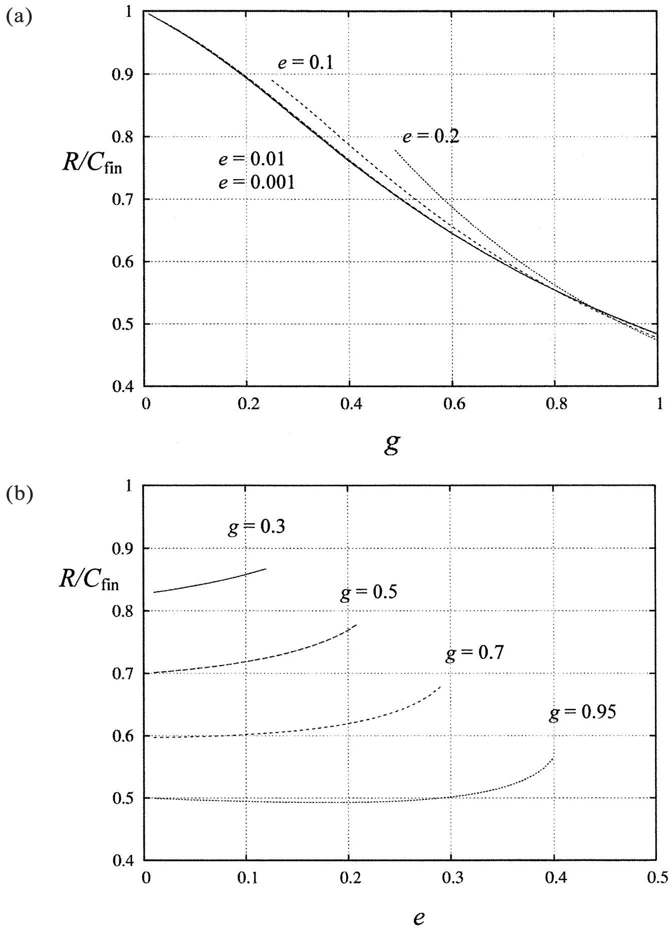

Fig. 5. (a) Fraction of reheated chondrules R/C_{fin} as a function of the production efficiency g. (b) Fraction of reheated chondrules R/C_{fin} as a function of the destruction efficiency e.

It seems that more than a half of chondrules should have experienced multiple heating events. Petrographic studies of chondrules show that at least 15% of chondrules show clear evidence for multiple heating events (Jones, 1996; Rubin and Krot, 1996). Tachibana *et al.* (2003) showed that four out of sixteen ferromagnesian UOC chondrules may have experienced multiple heating, and Tomomura *et al.* (2004) have found relict grains in ~10% of chondrules they observed. Considering that there would be more chondrules where recycling could not be identified from petrologic observation, the observed fraction (~10–25%) should be regarded as the minimum value. Thus, our estimate of >50% is consistent with the observation and seems a fairly reasonable value.

4.3. Age distribution of chondrules

The age distribution of chondrules, $y(t)$, is dependent on the time variation of the rate of heating events $h(t)$. We calculate $y(t)$ for different time-evolution paths of $h(t)$ and compare the calculated $y(t)$ with the estimated age-distribution of natural chondrules seen in Fig. 2. The time evolutions of $h(t)$ examined in this study are as follows: for $t_0 \leq t \leq t_{\mathrm{fin}}$,

case 1: constant,

$$h(t) = h_0,$$

case 2: linearly declining,

$$h(t) = -2h_0 \cdot \left(t/t_{\mathrm{fin}} - 1\right),$$

case 3: sinusoidal with a peak,

$$h(t) = h_0\left(1 - \cos\frac{2\pi(t - t_0)}{t_{\mathrm{fin}} - t_0}\right),$$

and

case 4: exponential decreasing,

$$h(t) = h_0(e^{-a(t/t_{\mathrm{fin}}-1)} - 1),$$

and $h(t) = 0$ for $t < t_0$ and $t_{\mathrm{fin}} < t$, where h_0 is a positive constant determined by the total amount of heating and a is a positive constant which is set to be 3 in this study, unless it is stated otherwise (Fig. 9). In cases 2, 3, and 4, the rate $h(t)$ becomes zero at $t = t_{\mathrm{fin}}$.

The characteristics of the estimated age-distribution of natural chondrules that we attempt to explain are that the time of the peak is 1.8 Myr and that the times when the distribution becomes half of the maximum are 1.5 Myr and 2.1 Myr. The best values of the starting and ending times of the chondrule formation epoch, t_0 and t_{fin}, are sought to fit these conditions.

Best-fit age-distributions ($\int_{t_i - 0.1\,\mathrm{Myr}}^{t_i + 0.1\,\mathrm{Myr}} y(t)\,\mathrm{d}t \Big/ \int_{0\,\mathrm{Myr}}^{3\,\mathrm{Myr}} y(t)\,\mathrm{d}t$, $t_i = i \times 0.2$ Myr, $i = 0, 1, 2, \cdots, 15$) for different $h(t)$ (cases 2, 3, and 4) are displayed in Fig. 6a. The best-fit rate of heating events $h(t)$ for each case is displayed in Fig. 6b. Best fit values of t_0 and t_{fin} are listed in Table 2a. The formation and destruction efficiencies are assumed to be $g = 0.5$

Table 2. Best fit of the starting and ending times for the chondrule forming epoch.

Case	t_0 [Myr]	t_{fin} [Myr]
(a) Condition A: $g = 0.5$, $e = 0.1$		
2: linear	1.2	2.2
3: sinusoidal	0.6	2.3
4: exponential	1.3	2.3
(b) Condition B (more productive): $g = 0.8$, $e = 0.01$		
2: linear	1.5	2.2
3: sinusoidal	1.0	2.3
4: exponential	1.5	2.3
(c) Condition C (less productive) case: $g = 0.5$, $e = 0.2$		
2: linear	1.0	2.2
3: sinusoidal	0.4	2.3
4: exponential	1.15	2.25

and $e=0.1$ in the model calculations, which lead the total amount of heating to be 3.05 (condition A). The age distributions in the model seem to reproduce well the estimated age distribution of chondrules (Fig. 2). The age distribution for a constant h (case 1) is not shown in Fig. 6a because it increases monotonically with time and cannot reproduce the peak at 1.8 Myr. It is seen in Fig. 6b that the ending time of the chondrule formation (t_{fin}) is 2.2–2.3 Myr after the CAI formation. One prominent feature of the model rates of heating events in Fig. 6b is that the evolutions of $h(t)$ after the peak ($1.8\,\mathrm{Myr}<t$) are almost the same (monotonic decreasing), while they are different before the peak age ($t<1.8\,\mathrm{Myr}$). This implies that the inferred evolution of $h(t)$ at $1.8\,\mathrm{Myr}<t$ is reliable. Although it is difficult to evaluate the time variation of heating events at $t<1.8\,\mathrm{Myr}$ from the chondrule age-distribution due to age-resetting by reheating events, the model suggests that the peak of the heating event rate should be 1.2–1.5 Myr after the CAI formation, 0.3–0.6 Myr earlier than the peak of the estimated

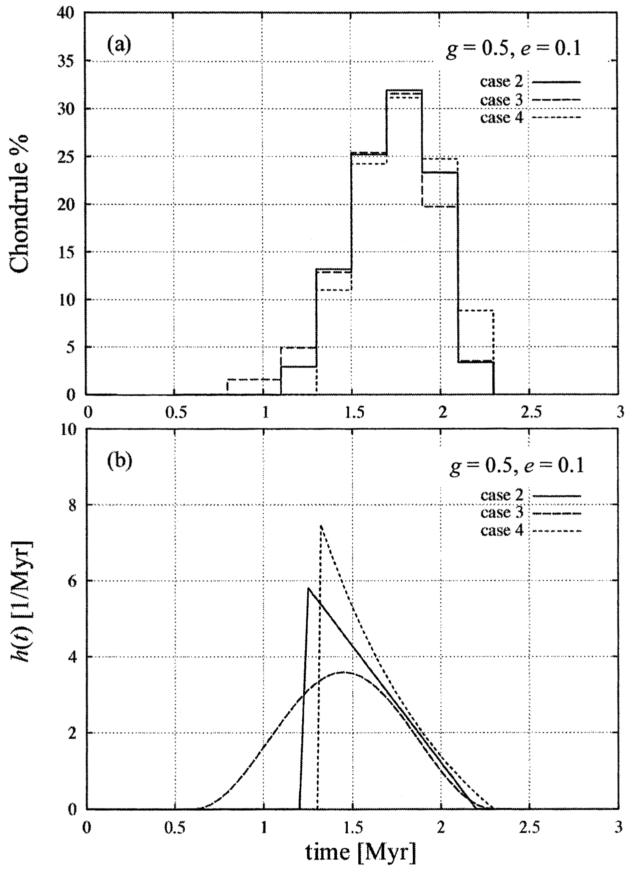

Fig. 6. Best-fit model age distributions and rate of heating events with the production efficiency $g=0.5$ and the destruction efficiency $e=0.1$. The evolutions of all the cases shown here after 1.8 Myr (age peak) are almost the same. The peak of the heating event rate is 0.3–0.5 Myr earlier than the peak of the age distribution.

age distribution of chondrules ($t = 1.8$ Myr). The total duration of chondrule forming events is thus 0.7–1.1 Myr. It should also be noted that our model implies that the age-distribution should have a peak earlier than $t = 1.8$ Myr if chondrule formation started as early as $t = 0$ Myr, indicating that there would be a time-gap between CAI- and chondrule-forming events. This implies that CAIs and chondrules formed not only under different conditions but by different heating mechanisms.

The dependence of the model age-distribution on the formation and destruction efficiencies (g and e) is also evaluated. Figure 7 shows the calculated age distributions (panel a) and the evolutions of the rate of heating events, $h(t)$, (panel b) for a more productive case with the efficiencies $g = 0.8$ and $e = 0.01$ (condition B). Thus, the total amount of heating required for $C_{\rm fin} = 0.7$ is 1.52, which is smaller than that required for condition A. The best fitting time parameters t_0 and $t_{\rm fin}$ are listed in Table 2b. The peak of the heating event rate ($h(t)$) is 0.1–0.3 Myr earlier than the peak of chondrule age distribution (1.4–1.7 Myr after CAIs), while the ending time of 2.2–2.3 Myr after CAIs is almost the same as that for condition A. The duration of chondrule formation

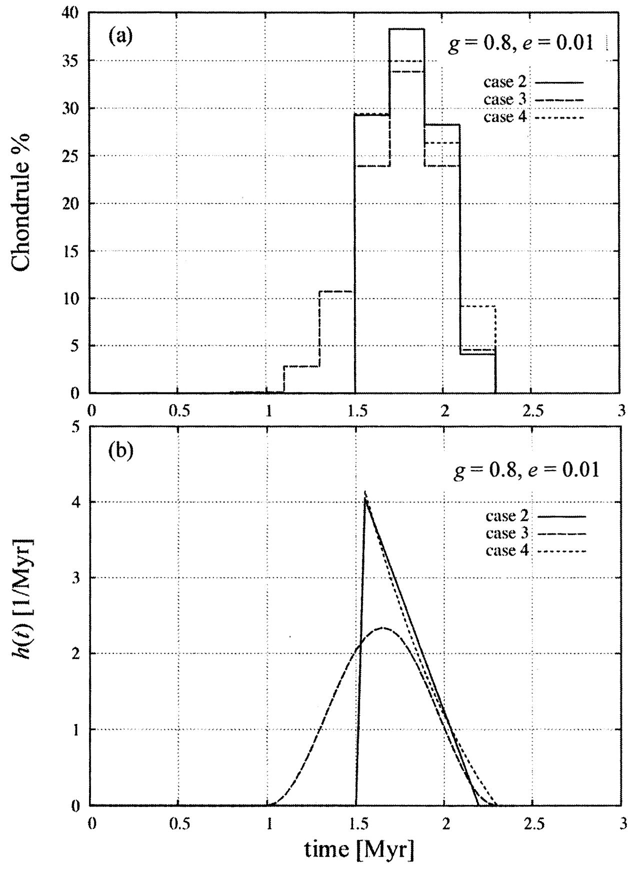

Fig. 7. Best-fit model age distributions and rate of heating events evolutions for the production efficiency $g = 0.8$ and the destruction efficiency $e = 0.01$.

is thus shorter (0.5–0.8 Myr) than that for condition A. This is due to effective formation of chondrules (large g and small e).

Figure 8 displays the age distributions with $g=0.5$ and $e=0.2$ (condition C), which represents a less productive condition than condition A. The total amount of heating for $C_{\text{fin}}=0.7$ is 5.59, which is larger than that for condition A. The best fitting time parameters are listed in Table 2c. The peak of the heating events ($h(t)$) is 0.5–0.8 Myr earlier than that for chondrule age distribution (1.0–1.3 Myr after CAIs). On the other hand, as in conditions A and B, the ending time of heating events is 2.2–2.3 Myr after CAIs. The duration of chondrule forming events (1.0–1.2 Myr) is longer than those for conditions A and B due to less efficient chondrule formation.

In order to see effects of late heating, we examined the chondrule age distribution with the condition A, but $a=13$ in the exponential decreasing case (case 4). (Note that the value of a in other calculations was $a=3$.) Results are shown in Fig. 9 along with results with case 2 and 3. Best fit parameters are $t_0=1.5$ Myr and $t_{\text{fin}}=3.0$ Myr, re-

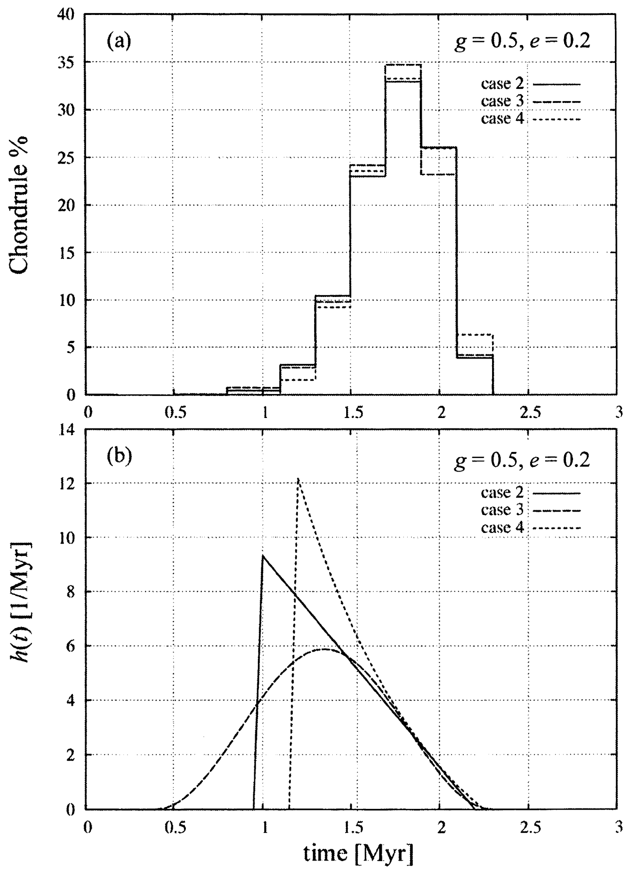

Fig. 8. Best-fit model age distributions and rate of heating events evolutions for the production efficiency $g=0.5$ and the destruction efficiency $e=0.2$.

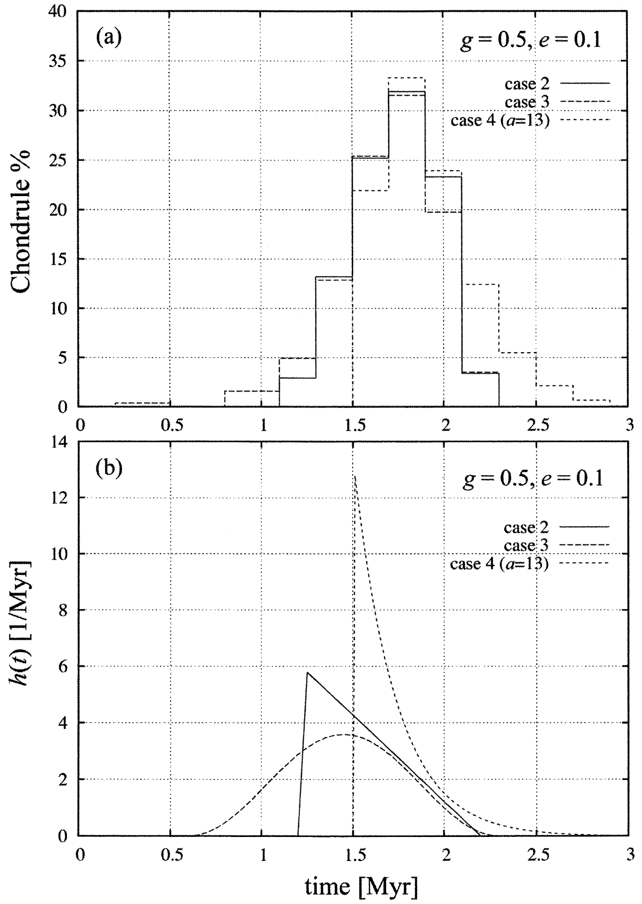

Fig. 9. Best-fig model age distributions and rate of heating events evolutions. Conditions ($g=0.5$ and $e=0.1$) and cases (functional forms of $h(t)$) are the same with those of Fig. 6 except for $a=13$, which corresponds to the decaying time scale of the exponentially decreasing rate in case 4. The final time of the heating events becomes $t_{\text{fin}}=3.0$ Myr and some young chondrules (ages >2.3 Myr) are present. However, a major part of the distribution is not altered from the one in Fig. 6.

spectively. Again, we can see that the rates of heating events, $h(t)$, of three cases at around $t=2.0$ Myr are very similar. Comparing with Fig. 6, we can also see that young chondrules are more present than results in Fig. 6, but the fraction of those young chondrules is rather small. This is because the rate of heating events after 2 Myr is very low; after $t=2.3$ Myr, $h(t)$ is virtually $h(t)=0$. Thus, the late heating, which lasted even after 2.3 Myr and formed young chondrules (ages >2.3 Myr), does not seem to have any significant effect on our results shown in Figs 6, 7, and 8.

Our calculations for different chondrule-forming efficiencies suggest that chondrule formation may have started at $t>0$ and may have almost ceased at $t=2.2$–2.3 Myr after CAIs, implying that the heating events for chondrules might be different from the

CAI-forming heating events.

4.4. Physical nature of efficiencies g and e

The formation and destruction efficiencies, g and e, affect the time evolution of the best-fit rate of heating events and the calculated age distribution. Hence, physically reliable origin of those efficiencies should be clarified to reveal the nature of the chondrule-forming heating events, though it seems not easy to address. Here, we discuss only some basic points on the nature of those efficiencies. It is obvious that further studies should be conducted in the future.

When chondrules were formed by melting of fine dust particles, at least the following processes would have taken place. Dust coagulates would have grown to about 1 mm in size due to collision and coalescence. Such dust aggregates would have been heated and melted by heating events to form chondrules. The formation efficiency g is a product of all the efficiencies of those sequential processes above. Coagulation and growth of dust particles may have been very efficient. The time scale of dust growth to mm size is estimated to be of the order of 10^4 yr at a region 1 AU from the Sun in the minimum mass solar nebula model if there is no turbulence (Nakagawa *et al.*, 1981). According to the results obtained in Section 4.3, heating events for a single dust particle would take place a few or several times in about one million years. This means that an average interval between each heating event for a dust particle is of the order of 10^5 yr, which is longer than the time scale of grain growth. Thus, dust particles may have become large enough to form chondrules before the next heating event.

Shock wave heating has been proposed to be responsible for melting of chondrule precursors (*e.g.*, Hood and Horanyi, 1991; Iida *et al.*, 2001). If this is the case, the strength of the shock wave can change the efficiency g; if the shock wave was not strong, dust particles would not be heated enough to form chondrules, while if the shock wave was too strong, dust particles may have evaporated completely (Iida *et al.*, 2001; Miura *et al.*, 2002).

The destruction efficiency e during shock wave heating may depend on following factors: destruction of chondrules due to collisions with other dust particles, incorporation into a larger (probably non-chondrule) dust particle by collision (*i.e.*, grain growth), evaporation due to reheating processes, and so forth. The first and second processes depend on the strength of the projectile and the velocity. Although the basic physics of such processes (*e.g.*, outcomes of dust-dust collisions) have been examined intensively by theoretical and experimental methods, the real number density of dust particles and the velocity distribution in the chondrule forming region are not easy to be estimated. As for destruction by evaporation (complete evaporation) during shock wave heating, almost no research has been done so far.

Note that the efficiencies g and e might have varied with time although they are assumed to be constant in this study for simplicity. The calculations above should be discussed with time dependent g and e in the future to reveal the nature of the chondrule formation process in detail.

5. Conclusions

In order to obtain a general picture of chondrule forming events in the early solar system, we have estimated the age distribution of natural chondrules in LL3.0–3.1 unequilibrated ordinary chondrites and have developed a simple phenomenological chondrule formation model, where chondrules are formed in a closed system in which dust and chondrules coexist, to explain the estimated age distributions.

1) The estimated ages of chondrules in LL3.0–3.1 chondrites range from 1 Myr to 3 Myr after the CAI formation with a peak around 1.8 Myr.

2) The estimated age distribution indicates that each event heated only a small fraction of dust material in the chondrule-forming region and numerous heating events are necessary to produce abundant chondrules in ordinary chondrites.

3) The average number of heating events experienced by a dust particle in our model is more than 1.2, which depends on the efficiencies of formation and destruction of chondrules during the heating process.

4) The model suggests that more than a half of the chondrules have been reheated.

5) The age distribution was well reconstructed by three types of rates of heating events, $h(t)$, *i.e.*, linearly decreasing, sinusoidal with a peak, and exponentially declining functions of time. The starting and ending timings of chondrule formation are 0.4–1.5 Myr and 2.2–2.3 Myr after CAIs, depending on the type of the function. The total duration of chondrule formation is thus 0.7–1.9 Myr.

6) In order to reproduce the age distribution of chondrules, $h(t)$ should decrease monotonically with time after the peak of the age distribution (1.8 Myr after CAIs) in three types of $h(t)$ described above.

7) The peak of $h(t)$ was 0.1–0.8 Myr earlier than the peak of the age distribution of chondrules, depending on the chondrule forming efficiency.

8) Chondrule-forming heating events seem to have started about 0.4 Myr or more after the CAI formation, implying that chondrule formation events were different from CAI formation events.

Acknowledgments

Authors would like to thank Dr. Connolly and an anonymous reviewer for their helpful comments to the original manuscript. TN was supported by Grant-in-Aid for Young Scientists (B) (14740284) of Japan Society for the Promotion of Science.

References

Amelin, Y., Krot, A.N., Hutcheon, I.D. and Ulyanov, A.A. (2002): Lead isotopic ages of chondrules and calcium-aluminum-rich inclusions. Science, **35**, 859–868.

Bizzaro, M., Baker, J.A. and Haack, H. (2004): Mg isotope evidence for contemporaneous formation of chondrules and refractory inclusions. Nature, **431**, 275–278.

Boss, A.P. (1996): A concise guide to chondrule formation models. Chondrules and the Protoplanetary Disk, ed. by R.H. Hewins *et al*. Cambridge, Cambridge Univ. Press, 257–263.

Boss, A.P. and Graham, J.A. (1993): Clumpy disk accretion and chondrule formation. Icarus, **106**, 168–178.

Ciesla, F.J. and Hood, L.L. (2002): The nebular shock wave model for chondrule formation: shock processing in a particle-gas suspension. Icarus, **158**, 281–293.

Connolly, H.C., Jr. and Love, S.G. (1998): The formation of chondrules: Petrologic tests of the shock wave model. Science, **280**, 62–67.

Desch, S.J. and Connolly, H.C., Jr. (2002): A model of the thermal processing of particles in solar nebula shocks: Application to the cooling rates of chondrules. Meteorit. Planet. Sci., **37**, 183–207.

Eisenhour, D.D., Daulton, T.L. and Buseck, P.R. (1994): Electromagnetic heating in the early solar nebula and the formation of chondrules. Science, **265**, 1067–1070.

Grossman, J.N., Rubin, A.E., Nagahara, H. and King, E.A. (1988): Properties of chondrules. Meteorites and the Early Solar System, ed. by J.F. Kerridge and M.S. Matthews. Tucson, Univ. Arizona Press, 619–659.

Hood, L.L. (1998): Thermal processing of chondrule precursors in planetesimal bow shocks. Meteorit. Planet. Sci., **33**, 97–107.

Hood, L.L. and Horanyi, M. (1991): Gas dynamic heating of chondrule precursor grains in the solar nebula. Icarus, **93**, 259–269.

Hood, L.L. and Horanyi, M. (1993): The nebular shock wave model for chondrule formation: One-dimensional calculations. Icarus, **106**, 179–189.

Hood, L.L. and Kring, D.A. (1996): Models for multiple heating mechanisms. Chondrules and the Protoplanetary Disks, ed. by R.H. Hewins *et al*. Cambridge, Cambridge Univ. Press, 265–276.

Hutcheon, I.D. and Hutchison, R. (1989): Evidence from the Semarkona ordinary chondrite for Al-26 heating of small planets. Nature, **337**, 238–241.

Huss, G.R., MacPherson, G.J., Wasserburg, G.J., Russell, S.S. and Srinivasan, G. (2001): ^{26}Al in CAIs and chondrules from unequilibrated ordinary chondrites. Meteorit. Planet. Sci., **36**, 975–997.

Iida, A., Nakamoto, T., Susa, H. and Nakagawa, Y. (2001): A shock heating model for chondrule formation in a protoplanetary disk. Icarus, **153**, 430–450.

Jones, R.H. (1990): Petrology and mineralogy of Type II, FeO-rich chondrules in Semarkona (LL3.0)—Origin by closed-system fractional crystallization, with evidence for supercooling. Geochim. Cosmochim. Acta, **54**, 1785–1802.

Jones, R.H. (1994): Petrology of FeO-poor, porphyritic pyroxene chondrules in the Semarkona chondrite. Geochim. Cosmochim. Acta, **58**, 5325–5340.

Jones, R.H. (1996a): FeO-rich, porphyritic pyroxene chondrules in unequilibrated ordinary chondrites. Geochim. Cosmochim. Acta, **60**, 3115–3138.

Jones, R.H. (1996b): Relict grains in chondrules: Evidence for chondrule recycling. Chondrules and the Protoplanetary Disk, ed. by R.H. Hewing *et al*. Cambridge, Cambridge Univ. Press, 163–172.

Jones, R.H. and Scott, E.R.D. (1989): Petrology and thermal history of type IA chondrules in the Semarkona (LL3.0) chondrite. Lunar and Planetary Science XIX. Houston, Lunar Planet. Inst., 523–536.

Jones, R.H., Lee, T., Connolly, H.C., Jr., Love, S.G. and Shang, H. (2000): Formation of chondrules and CAIs: Theory *vs*. observation. Protostars and Planets IV, ed. by V. Mannings *et al*. Tucson, Univ. Arizona Press, 927–962.

Kita, N.T., Nagahara, H., Togashi, S. and Morishita, Y. (2000): A short duration of chondrule formation in the solar nebula: evidence from ^{26}Al in Semarkona ferromagnesian chondrules. Geochim. Cosmochim. Acta, **64**, 3913–3922.

Kita, N.T., Ikeda, Y., Shimoda, H., Morishita, Y. and Togashi, S. (2003): Timing of basaltic volcanism in ureilite parent body inferred from the ^{26}Al ages of plagioclase-bearing clasts in DaG-319 polymict ureilite. Lunar and Planetary Science XXXIV. Houston, Lunar Planet. Inst., Abstract #1557 (CD-ROM).

Kita, N.T., Tomomura, S., Tachibana, S., Nagahara, H. and Morishita, Y. (2005): Correlation between aluminum-26 ages and bulk Si/Mg ratios for chondrules from LL3.0–3.1 chondrites. Lunar and Planetary Science XXXVI. Houston, Lunar Planet. Inst., Abstract #1750 (CD-ROM).

Liffman, K. (1992): The formation of chondrules via ablation. Icarus, **100**, 608–620.

MacPherson, G.J., Hashimoto, A. and Grossman, L. (1985): Accretionary rims on inclusions in the Allende meteorite. Geochim. Cosmochim. Acta, **49**, 2267–2279.

McKeegan, K.D., Greenwood, J.P., Leshin, L.A. and Cosarinsky, M. (2000): Abundance of ^{26}Al in ferromagnesian chondrules of unequilibrated ordinary chondrites. Lunar Planetary Science XXXI.

Houston, Lunar Planet. Inst., Abstract #2009 (CD–ROM)
Miura, H. and Nakamoto, T. (2005a): A shock-wave heating model for chondrule formation II: Minimum size of chondrule precursors. Icarus (in press).
Miura, H. and Nakamoto, T. (2005b): Thermal history of chondrules during shock-wave heating. Antarct. Meteorite Res., **18**, 239–252.
Miura, H., Nakamoto, T. and Susa, H. (2002): A shock-wave heating model for chondrule formation: Effects of evaporation and gas flows on silicate particles. Icarus, **160**, 258–270.
Morfill, G., Spruit, H. and Levy, E.H. (1993): Physical processes and conditions associated with the formation of protoplanetary disk. Protostars and Planets III, ed. by E.H. Levy and J.I. Lunine. Tucson, Univ. Arizona Press, 939–978.
Mostefaoui, S., Kita, N.T., Togashi, S., Tachibana, S., Nagahara, H. and Morishita, Y. (2002): The relative formation ages of ferromagnesian chondrules inferred from their initial aluminum-26/aluminum-27 ratios. Meteorit. Planet. Sci., **37**, 421–438.
Nagahara, H. (1981): Evidence for secondary origin of chondrules. Nature, **292**, 135–136.
Nakagawa, Y., Nakazawa, K. and Hayashi, C. (1981): Growth and sedimentation of dust grains in the primordial solar nebula. Icarus, **45**, 517–528.
Rubin, A.E. (1999): Troilite in the chondrules of type-3 ordinary chondrites: Implications for chondrule formation. Geochim. Cosmochim. Acta, **63**, 2281–2298.
Rubin, A.E. and Krot, A.N. (1996): Multiple heating of chondrules. Chondrules and the Protoplanetry Disk, ed. by R.H. Hewing *et al*. Cambridge, Cambridge Univ. Press, 173–180.
Russell, S.S., Srinivasan, G., Huss, G.R., Wasserburg, G.J. and MacPherson, G.J. (1996): Evidence for widespread ^{26}Al in the solar nebula and constraints for nebula time scales. Science, **273**, 757–762.
Sekiya, M., Uesugi, M. and Nakamoto, T. (2003): Flow in a liquid sphere moving with a hypersonic velocity in a rarefied gas—An analytic solution of the linearized equations—. Progr. Theor. Phys., **109**, 717–728.
Stolper, E. and Paque, J.M. (1986): Crystallization sequences of Ca-Al-rich inclusions from Allende: The effects of cooling rate and maximum temperature. Ceochim. Cosmochim. Acta, **50**, 1785–1806.
Shu, F.H., Shang, H. and Lee, T. (1996): Toward an astrophysical theory of chondrites. Science, **271**, 1545–1552.
Susa, H. and Nakamoto, T. (2002): On the maximal size of chondrules in shock-wave heating model. Astrophys. J., **564**, L57–L60.
Tachibana, S., Nagahara, H., Mostefaoui, S. and Kita, N.T. (2003): Correlation between relative ages inferred from ^{26}Al and bulk compositions of ferromagnesian chondrules in least equilibrated ordinary chondrites. Meteorit. Planet. Sci., **38**, 939–962.
Tanaka, K.K., Tanaka, H., Nakazawa, K. and Nakagawa, Y. (1998): Shock heating due to accretion of a clumpy cloud onto a protoplanetary disk. Icarus, **134**, 137–154.
Tomomura, S. (2004): Important constraints on the formation of chondrules inferred from the diversity of bulk chemical composition in the least equilibrated ordinary chondrites. Master Thesis, Univ. Tokyo.
Tomomura, S., Nagahara, H., Tachibana, S., Kita, N.T. and Morishita, Y. (2004): Relationship between bulk chemical composition and formation age of chondrules in Bishunpur and Krymka. Lunar Planetary Science XXXV. Houston, Lunar Planet. Inst., Abstract #1555 (CD-ROM).
Weidenschilling, S.J., Marzari, F. and Hood, L.L. (1998): The origin of chondrules at jovian resonances. Science, **279**, 681–684.
Wood, J.A. (1962): Chondrules and the origins of the terrestrial planets. Nature, **194**, 127–130.
Zinner, E. and Göpel, C. (2002): Aluminum-26 in H4 chondrites; Implications for its production and its usefulness as a fine-scale chronometer for early solar system events. Meteorit. Planet. Sci., **37**, 1001–1013.